A TWO PHASE FLOW MODEL OF THE RAYLEIGH-TAYLOR MIXING ZONE *

Yupin Chen, James Glimm, † David H. Sharp, Qiang Zhang
The University at Stony Brook, Stony Brook, NY 11794-3600

Abstract

The Rayleigh-Taylor instability of an interface separating fluids of distinct density is driven by an acceleration across the interface. Low order statistical moments of fluctuating fluid quantities characterize the hydrodynamics of the mixing zone.

A new model is proposed for the momentum coupling between the two phases. This model is validated against computational data for compressible flows, including flows near the incompressible limit. Our main result is a zero parameter first order closure for ensemble averaged two phase flow equations. We do not, however, fully solve the closure problem, as the equations we derive are missing an (internal) boundary condition along any surface for which either phase goes to zero volume fraction. In this sense, the closure problem is reduced from a volume to a surface condition, rather than being solved completely.

A new understanding of the compressibility dependent loss of universality of the mixing rate is obtained in terms of a one parameter family of solutions of the two phase flow equations. This parameter measures the initial perturbation amplitude in dimensionless units which eliminate this effect in the incompressible limit.

We compare two formulations of the statistical moments, one based on two phase flow and the other on turbulence models. These formulations describe different aspects of the mixing process. For the problem considered, the two phase flow moments appear to be preferable, in that they subsume the turbulence moments but not conversely.

*Supported by the Applied Mathematics Subprogram of the U.S. Department of Energy DE-FG02-90ER25084.

†Also supported by the Army Research Office, grant DAAL03-92-G-0185 and through the Mathematical Sciences Institute of Cornell University under subcontract to the University at Stony Brook, ARO contract number DAAL03-91-C-0027, and the National Science Foundation, grant DMS-9201581.

AMS (MOS) Subject Classification:
Key words: Rayleigh-Taylor, multiphase, turbulence.

1 Introduction

We study ensemble averaged equations for multi-fluid mixing. Ensemble averaging, for nonlinear equations generally and for fluid flow equations specifically, introduces new variables, requiring new equations, and a hierarchy of higher order moments and equations. This hierarchy is usually broken at the level of first or second order moments by a closure hypothesis, which relates the higher order moments occurring in the equations to products of lower order moments, already having a dynamical equation. The closure hypothesis can be viewed as an approximation, or as a type of physical law, descriptive of the context to which it applies. We prefer the latter view, as with thermodynamics, and think of closure as a type of constitutive law or equation of state description characterizing *e.g.* turbulence or multiphase flow, with a specific closure hypothesis valid for some flow regimes, but not others.

The flow regime studied here is the mixing layer associated with the Rayleigh-Taylor instability [11] in which a light fluid acts via an external force (gravity) to accelerate a heavy one. The data required to validate our closure hypothesis comes from the experimental measurement of rocket accelerated fluid interfaces [10,14], and from numerical simulations of the two fluid Euler equations by the front tracking method [2,6,7]. Among the many numerical studies of Rayleigh-Taylor instability, *e.g.* [4,13,14], the front tracking simulations appear to be distinguished in their ability to include compressible effects and to agree with incompressible laboratory experiments in the incompressible limit. For this reason, they provide a suitable data set for validation of our closure hypothesis.

Among our main results is the derivation and validation of a new first order closure for compressible multiphase flow. The dependent variables are the ensemble averages of the volume fraction and the density, momentum, and energy in each phase. For such a system the phase pressure is a function of the thermodynamic variables in its own phase. The problem of formulating an equation of state for the mixed phase is thereby circumvented. This is achieved at the expense of enlarging the number of dependent variables employed. The use of additional variables also allows a more fundamental description of the momentum coupling between the two phases. Our solution of the closure problem is not complete: there is a missing boundary condition along surfaces for which the volume fraction of one of the two phases goes to zero. In the interior of the mixing zone, where the

phase volume fractions are bounded away from zero and one, the closure is complete; moreover, in this region, the closure has no free parameters. It avoids the use of a phenomenological length scale with its own equation of motion in order to formulate a "drag term". We speculate, however, that a one parameter closure with "drag" may be useful at the edge of the mixing zone.

Our proposed equations are validated by derivation from fundamental two fluid Euler equations with all modeling or approximation steps justified by comparison to simulation data for the Rayleigh-Taylor problem, as well as by arguments of physical plausibility. Because the closure is not complete, we do not predict the overall mixing rate coefficient, α. The derivation we give is more satisfactory than the customary arguments based on the principle that two expressions which have the same physical dimensions will be equivalent up to a dimensionless constant. Conventional closures, with a phenomenological length scale and drag term, can be derived from ours.

We have previously noted a significant compressibility dependence [2] in the growth rate of the mixing zone, accompanied by a loss in universality in this quantity. We provide here a new understanding of these phenomena. There is a one parameter family of solutions to our multiphase flow equations, parametrized by a dimensionless measure of the initial amplitude. The non-dimensionalization maps all initial conditions into a single point in the incompressible limit, which explains the occurrence of an incompressible fixed point and the loss of universality in the compressible case. The dependence of our solutions on the initial ensemble can also be understood in terms of the relative weighting of short and moderate wavelength perturbations. (Long wavelength perturbations have been systematically excluded in this study.) Again, the nondimensionalization has the property of eliminating this ensemble dependence in the incompressible limit.

We also compare alternative closure possibilities. We compare first order multiphase moments to second order turbulent moments. We find, to good approximation for this data set, that the second order turbulence moments can be expressed as products of first order multiphase moments. On this basis, we regard the multiphase description and closure as the more satisfactory of the two for this data set.

2 Turbulence Moments Derived from Two Phase Moments

The purpose of this section is to compare two phase mixing with turbulence modeling in the context of a data set which contains both mixing and turbulence aspects. We derive a formula relating turbulence moments to the corresponding two phase mixing quantities, and thereby differentiate between two mechanisms contributing to the turbulence moments.

We consider flow with no microscopic mixing, *i.e.* with a well defined two phase flow. We consider a problem in two space dimensions (x, z) at time t, which has an x direction symmetry, so that the ensemble average $\langle\cdot\rangle$ is independent of x.

The ensemble average is defined by a measure on the function space of initial conditions. The details are given in [2]. Briefly, the initial conditions are defined with periodic boundary conditions and with discrete Fourier modes having wavenumbers in the interval $k_{\min} \le k \le k_{\max}$. By convention, we have taken $k_{\max} = 2k_{\min}$ to suppress long wavelength disturbances. In this range, the Fourier amplitudes are independent Gaussian random variables. The expected value of the amplitude of each mode is small enough to be within the linear regime. For this reason, the initial amplitudes can be propagated backward or forward in time on the basis of the linear theory. Since the large k modes grow more rapidly than the small k modes, the assumption of equal amplitude of the distinct Fourier modes can be valid for at most one unique time in the evolution. Thus the overall amplitude of the modes, or the relative weighting of low to high frequencies, is a potentially significant parameter characterizing the ensemble. We return to this point in Section 5.

Let X_k be the characteristic function of the set in which fluid of phase k is located, and let $\alpha_k = \langle X_k \rangle$ be the volume fraction for phase k. Then α_k is a function of z, t but not a function of x. Let $\alpha = \alpha_1$, so that $1 - \alpha = \alpha_2$. For a quantity $a = a(x, z, t)$, we introduce the absolute and phase volume averages

$$\bar{a} = \langle a \rangle \ , \quad \bar{a}_k = \frac{\langle a X_k \rangle}{\langle X_k \rangle} = \frac{\langle a X_k \rangle}{\alpha_k} \ , \tag{2.1}$$

which are functions of z and t, and the absolute and phase fluctuating quantities

$$\delta a = a - \bar{a} \ , \quad \delta a_k = a - \bar{a}_k \ .$$

From these definitions, it follows that $\bar{a} = \alpha_1 \bar{a}_1 + \alpha_2 \bar{a}_2$.

The main result of this section is an expression of the second moments for the absolute fluctuating quantities in terms of the second moments of the phase fluctuating quantities plus an expression involving only the two phase first moments, *i.e.* the phase volume averages. Moreover, for a computational data set derived from Rayleigh-Taylor mixing, we show that the first contribution is small, so that the absolute second moments are effectively given as functions of the two phase first moments. We consider the absolute second moments

$$B = \langle \delta\rho \delta\rho \rangle \ , \tag{2.2a}$$

$$\vec{A} = \langle \delta\rho \delta\vec{v} \rangle \ , \tag{2.2b}$$

$$R = \langle \rho \vec{v} \vec{v} \rangle - \frac{\langle \rho \vec{v} \rangle \langle \rho \vec{v} \rangle}{\langle \rho \rangle} \ . \tag{2.2c}$$

These quantities arise as additional independent variables (beyond those occurring in the Euler equations for the fluid flow) in turbulence modeling of ensemble averaged flow, see [1]. In particular, they arise from averaging nonlinear terms in the momentum equation. Correspondingly, the single phase version of these moments are defined to be

$$B_k = \frac{\langle X_k (\delta \rho_k)^2 \rangle}{\alpha_k} \ , \tag{2.3a}$$

$$\vec{A}_k = \frac{\langle X_k \delta \rho_k \delta \vec{v}_k \rangle}{\alpha_k} \ , \tag{2.3b}$$

$$R_k = \frac{\langle X_k \rho \vec{v} \vec{v} \rangle}{\alpha_k} - \frac{\langle X_k \rho \vec{v} \rangle^2}{\alpha_k \langle X_k \rho \rangle} \ . \tag{2.3c}$$

An elementary direct calculation leads to the formulas

$$B = \alpha_1 B_1 + \alpha_2 B_2 + \alpha_1 \alpha_2 (\bar{\rho}_2 - \bar{\rho}_1)^2 \ , \tag{2.4a}$$

$$A = \alpha_1 A_1 + \alpha_2 A_2 + \alpha_1 \alpha_2 (\rho_1 - \rho_2)(\bar{v}_1 - \bar{v}_2) \ . \tag{2.4b}$$

Here, we suppress the vector indices in A and v.

To derive (2.4a), we write

$$\delta \rho = \rho - \bar{\rho} = X_1 (\rho - \bar{\rho}) + X_2 (\rho - \bar{\rho})$$

$$= X_1 (\delta \rho_1 + \bar{\rho}_1 - \bar{\rho}) + X_2 (\delta \rho_2 + \bar{\rho}_2 - \bar{\rho}) \ .$$

Since $X_1 X_2 = 0$ and expectations which are linear in fluctuating quantities must vanish,

$$B = \langle X_1 (\delta \rho_1)^2 \rangle + \langle X_2 (\delta \rho_2)^2 \rangle + \alpha_1 (\bar{\rho}_1 - \bar{\rho})^2 + \alpha_2 (\bar{\rho}_2 - \bar{\rho})^2 \ .$$

Elementary algebra, using the identities $\alpha_1 + \alpha_2 = 1$, $\bar{\rho} = \alpha_1 \bar{\rho}_1 + \alpha_2 \bar{\rho}_2$, and the definition (2.3a), yields (2.4a).

Similarly, we have

$$\delta v = v - \bar{v} = X_1 (v - \bar{v}) + X_2 (v - \bar{v})$$

$$= X_1 (\delta v_1 + \bar{v}_1 - \bar{v}) + X_2 (\delta v_2 + \bar{v}_2 - \bar{v}) \ .$$

Substituting this identity together with the $\delta \rho$ identity in the definition for A yields (2.4b).

In order to derive the corresponding formulas for R, we introduce a notation for mass weighted averages. Mass weighted averages are presumably more fundamental than volume based ones, and, in the case of R, they lead to simple formulas. Let

$$\tilde{a}_k = \frac{\langle X_k \rho a \rangle}{\langle X_k \rho \rangle} = \frac{\bar{\rho a}_k}{\bar{\rho}_k}$$

Then

$$R = \left(\alpha_1 R_1 + \frac{\alpha_1 (\bar{\rho v}_1)^2}{\bar{\rho}_1} \right) + \left(\alpha_2 R_2 + \frac{\alpha_2 (\bar{\rho v}_2)^2}{\bar{\rho}_2} \right)$$
$$- \frac{1}{\bar{\rho}} \left(\alpha_1^2 (\bar{\rho v}_1)^2 + \alpha_2^2 (\bar{\rho v}_2)^2 + 2\alpha_1 \alpha_2 \bar{\rho v}_1 \bar{\rho v}_2 \right) \quad .$$

This can be simplified to yield

$$R = \alpha_1 R_1 + \alpha_2 R_2 + \alpha_1 \alpha_2 \frac{\bar{\rho}_1 \bar{\rho}_2}{\bar{\rho}} (\tilde{v}_1 - \tilde{v}_2)^2 \quad . \tag{2.4c}$$

More important than identities, such as the above, are simple approximations, valid for specific data sets. This is the issue to which we now turn. For the Rayleigh-Taylor two phase mixing data under study here, we show that the dominant contribution to the turbulent second moments comes from the two phase first moments (mean flow quantities). In this approximation, we have

$$B \approx B_{\text{ two phase}} \equiv \alpha_1 \alpha_2 (\bar{\rho}_2 - \bar{\rho}_1)^2 \quad , \tag{2.5a}$$

$$A \approx A_{\text{ two phase}} \equiv \alpha_1 \alpha_2 (\bar{\rho}_1 - \bar{\rho}_2)(\bar{v}_1 - \bar{v}_2) \quad , \tag{2.5b}$$

$$R \approx R_{\text{ two phase}} \equiv \alpha_1 \alpha_2 \frac{\bar{\rho}_1 \bar{\rho}_2}{\bar{\rho}} (\tilde{v}_1 - \tilde{v}_2)^2 \quad . \tag{2.5c}$$

Now we present the comparison between the exact results and the results of the two phase flow approximation. The results presented in this section are the statistical average of five runs with Atwood number $A_t = \frac{\rho_2 - \rho_1}{\rho_2 + \rho_1} = \frac{2}{3}$, and dimensionless compressibility $M^2 = \lambda g / c_h^2 = 0.5$. Here $\rho_i, i = 1, 2$, denotes the density of the two fluids at the interface, λ is the wavelength of the perturbation and c_h is the sound speed in the heavy fluid. A more detailed study, with systematic variation of both the Atwood number and M^2, will be included in the thesis of the first author; the conclusions are basically the same. Each run has a different seed for the initial random interface. In Figures 2.1a and 2.1b, we compare the exact and two phase approximate versions of B and A, for Rayleigh-Taylor mixing data. We see that the approximation is very close to the exact correlation for A and B. In Figure 2.2 we compare the exact value of R with the value of the two phase approximation $R_{\text{ two phase}}$. The comparison shows that the two phase approximation captures

most of the contribution, although the agreement is not as good as the ones shown in Figure 2.1 for B and A.

Averaging the nonlinear terms in the energy equation also introduces second moments of fluctuating quantities. Let e denote internal energy per unit volume, and ϵ internal energy per unit mass, so the $e = \rho\epsilon$. The averaged energy equation contains a divergence of

$$S = \langle ev \rangle - \frac{\langle e \rangle \langle \rho v \rangle}{\langle \rho \rangle} = \langle \rho \epsilon v \rangle - \bar{\rho}\tilde{\epsilon}\tilde{v} \quad . \tag{2.6}$$

In addition, it contains drag related terms resulting from the average of pressure and velocity gradients. The analysis [1] of these terms leads to the correlation

$$G = \langle \delta\rho \delta\epsilon \rangle \quad . \tag{2.7}$$

As above, we can define single phase versions of S and G,

$$S_k = \frac{\langle X_k e v \rangle}{\alpha_k} - \frac{\langle X_k e \rangle \langle X_k \rho v \rangle}{\alpha_k \langle X_k \rho \rangle} \tag{2.8}$$

and

$$G_k = \frac{\langle X_k \delta\rho_k \delta\epsilon_k \rangle}{\alpha_k} \quad . \tag{2.9}$$

Then

$$S = (\alpha_1 S_1 + \alpha_1 \bar{e}_1 \tilde{v}_1) + (\alpha_2 S_2 + \alpha_2 \bar{e}_2 \tilde{v}_2)$$
$$- \frac{1}{\bar{\rho}} \left(\alpha_1^2 \bar{e}_1 \bar{\rho}_1 \tilde{v}_1 + \alpha_2^2 \bar{e}_2 \bar{\rho}_2 \tilde{v}_2 + \alpha_1 \alpha_2 (\bar{e}_1 \bar{\rho}_2 \tilde{v}_2 + e_2 \bar{\rho}_1 \tilde{v}_1) \right) \quad .$$

This can be simplified to

$$S = \alpha_1 S_1 + \alpha_2 S_2 + \frac{\alpha_1 \alpha_2}{\bar{\rho}} \left(\bar{\rho}_2 \bar{e}_1 - \bar{\rho}_1 \bar{e}_2 \right) \left(\tilde{v}_1 - \tilde{v}_2 \right) \quad .$$

Following the treatment of A above, we also have

$$G = \alpha_1 G_1 + \alpha_2 G_2 + \alpha_1 \alpha_2 (\bar{\rho}_1 - \bar{\rho}_2)(\bar{\epsilon}_1 - \bar{\epsilon}_2) \quad .$$

As with A, B, and R, we introduce the approximations

$$S \approx S_{\text{ two phase}} \equiv \frac{\alpha_1 \alpha_2}{\bar{\rho}} \left(\bar{\rho}_2 \bar{e}_1 - \bar{\rho}_1 \bar{e}_2 \right) \left(\tilde{v}_1 - \tilde{v}_2 \right) \quad ,$$

and

$$G \approx G_{\text{ two phase}} \equiv \alpha_1 \alpha_2 (\bar{\rho}_1 - \bar{\rho}_2)(\bar{\epsilon}_1 - \bar{\epsilon}_2) \quad .$$

See Figures 2.3a-b for a comparison between the exact results and the results from two phase flow approximation of S and G, for Rayleigh-Taylor mixing data. These figures show that the two phase flow approximation for S and G is an excellent one.

From Figures 2.1-3, we conclude that two phase mean flow (two phase first moments) will give a very good description of the turbulent second moments, and thus that the mixing phenomena in this data set is dominated by two phase behavior rather than by turbulence.

3 Equations for Compressible Two Phase Flow

Equations for two phase flow are derived in two steps. The first is a mathematically exact averaging operation, which, due to the nonlinearity of the equations, introduces new unknowns (equations which do not close). The second step is a modeling step, in which some of the unknowns are declared to be new dependent variables, for which new equations (not closing) are derived as above, and then the remaining unknown quantities are approximated in terms of the original and new dependent variables. For incompressible flows, this process is described very elegantly by Drew [3]. Examples of compressible multiphase flow equations are given in [8,9]. We follow the formalism of [3], introduced in part in §2 as well.

The Lagrangian interface satisfies the exact microscopic equation

$$\frac{\partial X_k}{\partial t} + \vec{v}_{\rm int} \cdot \nabla X_k = 0 \quad . \tag{3.1}$$

where $\vec{v}_{\rm int}$ is the velocity of the (Lagrangian) interface. Note that only the normal component $\vec{v}_{\rm int} \cdot \vec{n}_k$ of $\vec{v}_{\rm int}$ is well defined, where $\vec{n}_k$ is the unit vector normal to the interface. We orient $\vec{n}_k$ pointing out of phase k, so that

$$\vec{v}_{\rm int} \cdot \nabla X_k = \vec{v}_{\rm int} \cdot \vec{n}_k \frac{\partial X_k}{\partial n_k} \quad , \tag{3.2}$$

where $\frac{\partial X_k}{\partial n_k}$ is a negative delta function, per unit length or area of interface surface, for phase k. Thus, we have, identically

$$\frac{\partial \alpha_k}{\partial t} + \langle \vec{v}_{\rm int} \cdot \vec{n}_k \frac{\partial X_k}{\partial n_k} \rangle = 0 \quad . \tag{3.3}$$

The averaged equations resulting from conservation of mass follow those of [3], with the simplification that, due to the absence of transfer of mass across the interface, the source term $\Gamma_k = 0$. Thus

$$\frac{\partial \alpha_k \bar{\rho}_k}{\partial t} + \nabla \cdot \alpha_k \bar{\rho}_k \tilde{v}_k = 0 \quad . \tag{3.4}$$

Our treatment of the momentum equation also follows [3], with the following changes: The external force, f, is specialized to $\rho\vec{g}$, where $\vec{g}$ denotes gravity. Cancellations due to the fact that the interface moves with the fluid velocity are imposed. Surface tension has been set to zero. Reynolds stress terms, omitted in [3], are included. The result, after averaging, is

$$\frac{\partial\langle X_k\rho v\rangle}{\partial t} + \nabla\cdot\langle X_k\rho vv\rangle = -\nabla\langle X_k p\rangle + \langle p\nabla X_k\rangle + \langle X_k\rho\vec{g}\rangle \quad . \tag{3.5}$$

Here p denotes the pressure, assumed to be continuous across the interface. Using the identity

$$\nabla\langle X_k p\rangle = \nabla\frac{\langle X_k p\rangle\alpha_k}{\alpha_k} = \nabla(\bar{p}_k\alpha_k) \tag{3.6}$$

we have

$$\frac{\partial\alpha_k\bar{\rho}_k\tilde{v}_k}{\partial t} + \nabla\cdot(\alpha_k\bar{\rho}_k\tilde{v}_k\tilde{v}_k) = -\nabla(\alpha_k\bar{p}_k) + \alpha_k\bar{\rho}_k\vec{g} + \langle p\nabla X_k\rangle - \nabla\cdot(\alpha_k R_k) \quad . \tag{3.7}$$

The energy equation is considered as an equation for $\rho\epsilon$. After insertion of the X_k factors, rearranging terms and averaging, we obtain the identity

$$\frac{\partial\langle X_k\rho\epsilon\rangle}{\partial t} + \nabla\cdot\langle X_k v\rho\epsilon\rangle = -\langle X_k p\nabla\cdot\vec{v}\rangle \quad ,$$

which can be rewritten as

$$\frac{\partial\alpha_k\bar{\rho}_k\tilde{\epsilon}}{\partial t} + \nabla(\alpha_k\bar{\rho}\tilde{\epsilon}_k\tilde{v}_k) = -\nabla(\alpha_k S_k) - \langle X_k p\nabla\cdot\vec{v}\rangle \quad . \tag{3.8}$$

We can express the average of the $p\nabla\cdot\vec{v}$ term on the right hand side as

$$-\langle X_k p\nabla\cdot\vec{v}\rangle = -\langle p\nabla\cdot(X_k\vec{v})\rangle + \langle p\vec{v}\cdot\nabla X_k\rangle \quad .$$

We rewrite the first term by adding and subtracting the product of the averages, to obtain

$$-\langle p\nabla\cdot(X_k\vec{v})\rangle = \langle(\bar{p}_k - p)\,\nabla\cdot(X_k\vec{v})\rangle - \bar{p}_k\langle\nabla\cdot(X_k\vec{v})\rangle. \tag{3.9}$$

Combining the above expressions yields the exact averaged energy equation

$$\frac{\partial\alpha_k\bar{\rho}_k\tilde{\epsilon}_k}{\partial t} + \nabla(\alpha_k\bar{\rho}_k\tilde{\epsilon}_k\tilde{v}_k) = -\nabla(\alpha_k S_k) - \bar{p}_k\nabla\cdot(\alpha_k\bar{v}_k) + \langle(\bar{p}_k - p)\,\nabla\cdot(X_k\vec{v})\rangle + \langle p\vec{v}\cdot\nabla X_k\rangle \quad . \tag{3.10}$$

Equation (3.9), which is a truncated correlation, has been analyzed numerically, see Fig. 3.1, and is found to be small.

4 Effective Equations for Rayleigh-Taylor Mixing Data

In this section, we model (*i.e.* propose) effective dynamical equations for the averaged Rayleigh-Taylor mixing data. Because of the horizontal translational symmetry of the problem the averaging, as implemented numerically, is two fold, containing both the ensemble average over the initial data and the translational average of physical quantities at the same height.

There are three terms in (3.3), (3.7) and (3.10) which are proportional to ∇X_k, namely $\langle \vec{v}_{\rm int} \cdot \nabla X_k \rangle$ in (3.3), $\langle p \nabla X_k \rangle$ in (3.7) and $\langle p\vec{v} \cdot \nabla X_k \rangle$ in (3.10). These terms represent the coupling between the two phases. Notice that ∇X_k is a delta function in the direction normal to the interface between the two phases. These terms are intrinsically defined in higher dimensions only. However, the horizontal average maps these higher dimensional quantities onto one-dimensional ones. Therefore, they can not be determined exactly in the effective one dimensional dynamical equation without knowing the exact solution in higher dimensions. In order to resolve the closure problem for the effective dynamical equations, we model these terms next.

The three interfacial terms can be expressed as $\langle f \nabla X_k \rangle$, where $f = \vec{v}_{\rm int}, p, p\vec{v}$. We define an effective interfacial quantity $f_{\rm eff}$ as $\langle f \nabla X_k \rangle = \langle f_{\rm int} \nabla X_k \rangle \equiv f_{\rm eff} \nabla \langle X_k \rangle$. Here $f_{\rm int}$ is f evaluated at the interface, due to the δ function property of ∇X_k.

As fluid of phase 1 begins to penetrate into phase 2, the frontier portion of that fluid occupies only a small volume and is near the interface. Therefore in that regime $\bar{f}_1$ is a good approximation for $f_{\rm eff}$. Similarly, $\bar{f}_2$ is a good approximation for $f_{\rm eff}$ in the regime where the fluid of phase 2 penetrates into phase 1. We interpolate these two approximations to obtain a model for $f_{\rm eff}$,

$$f_{\rm eff} \approx \alpha_1 \bar{f}_2 + \alpha_2 \bar{f}_1. \tag{4.1}$$

Equation (4.1) models the effective coupling between phases in our one dimensional effective equations. Therefore the three interfacial terms are modeled as

$$\langle \vec{v}_{\rm int} \cdot \nabla X_k \rangle \approx (\alpha_1 \bar{v}_2 + \alpha_2 \bar{v}_1) \cdot \nabla \alpha_k \ , \tag{4.2}$$

$$\langle p \nabla X_k \rangle \approx (\alpha_1 \bar{p}_2 + \alpha_2 \bar{p}_1) \cdot \nabla \alpha_k \ , \tag{4.3}$$

$$\langle p\vec{v} \cdot \nabla X_k \rangle \approx (\alpha_1 \bar{p}_2 \bar{v}_2 + \alpha_2 \bar{p}_1 \bar{v}_1) \cdot \nabla \alpha_k \ . \tag{4.4}$$

To interpret these equations physically we note that when summed over k each side of these approximate equations gives zero. Thus these terms represent interchange of volume, momentum and energy, respectively, between the two phases.

We now show that (4.3) represents both equilibrated pressure boundary conditions and drag. To see this, we write $\bar{p} = \alpha_1 \bar{p}_1 + \alpha_2 \bar{p}_2$, and compute

$$\alpha_1 \bar{p}_2 + \alpha_2 \bar{p}_1 = \bar{p} - (\alpha_2 - \alpha_1)(\bar{p}_2 - \bar{p}_1) = \bar{p} - (\alpha_2 - \alpha_1)[(\bar{p}_2 - \bar{p}) - (\bar{p}_1 - \bar{p})].$$

We interpret $\bar{p}$ as the equilibrated pressure. The second term is the net interface pressure force on phase k due to its interaction with phase $k' \neq k$. It is the amount of the interface force due to pressure deviations from the equilibrated pressure. With the present set of variables, this expression does not require further modeling to in order to obtain a closed system.

Both the normal velocity and pressure are continuous across the interface in the absence of the surface tension. The continuity of pressure and normal velocity are preserved in these approximations. Namely, as we add up the interfacial contributions from the two phases, they cancel each other. In Figures 4.1-3, we compare the approximations in Eqs. (4.2)-(4.4) with the numerical results for simulations with Atwood number $A_t = 2/3$, $M^2 = 0.5$ at times $t = 3, 6, 9$ and 12. These results are obtained from an ensemble average over four runs with different initial random interfaces. The results from the model agree very well with the numerical solutions. Since data for pressure is much smoother than data for the velocity, the approximation for the average of the interfacial pressure is better than for the interfacial velocity. Figures 4.1 and 4.3 are quite similar, due to the facts that they both contain interfacial velocity and that the interfacial pressure is smooth.

As in §2, we set $R_k = S_k = 0$. Also we make the approximation $\bar{v}_k \approx \tilde{v}_k$. Figure 4.4 shows that $\bar{v}_k$ and $\tilde{v}_k$ are almost the same. Combining these with the approximation for the interfacial terms and the fact from §3 that the truncated correlation in the energy equation is negligible, we obtain the following one dimensional effective equations for the Rayleigh-Taylor mixing data:

$$\frac{\partial \alpha_k}{\partial t} + (\alpha_1 \bar{v}_2 + \alpha_2 \bar{v}_1) \frac{\partial \alpha_k}{\partial z} = 0 \quad , \tag{4.5}$$

$$\frac{\partial \alpha_k \bar{\rho}_k}{\partial t} + \frac{\partial \alpha_k \bar{\rho}_k \bar{v}_k}{\partial z} = 0 \quad , \tag{4.6}$$

$$\begin{aligned} \frac{\partial \alpha_k \bar{\rho}_k \bar{v}_k}{\partial t} + \frac{\partial (\alpha_k \bar{\rho}_k \bar{v}_k \bar{v}_k)}{\partial z} &= -\frac{\partial (\alpha_k \bar{p}_k)}{\partial z} + \alpha_k \bar{\rho}_k g \\ &+ (\alpha_1 \bar{p}_2 + \alpha_2 \bar{p}_1) \frac{\partial \alpha_k}{\partial z} \quad , \end{aligned} \tag{4.7}$$

$$\frac{\partial (\alpha_k \bar{\rho}_k \tilde{\epsilon}_k)}{\partial t} + \frac{\partial (\alpha_k \bar{\rho}_k \tilde{\epsilon}_k \bar{v}_k)}{\partial z} = -\bar{p}_k \frac{\partial (\alpha_k \bar{v}_k)}{\partial z} + (\alpha_1 \bar{p}_2 \bar{v}_2 + \alpha_2 \bar{p}_1 \bar{v}_1) \frac{\partial \alpha_k}{\partial z} \quad , \tag{4.8}$$

for $k = 1, 2$ and

$$\alpha_1 + \alpha_2 = 1. \tag{4.9}$$

We next explain how the usual expression for drag in two phase flow can be derived from (4.7). Consider the first and third terms on the rhs of (4.7). These can be written as

$$-\alpha_k \frac{\partial \bar{p}_k}{\partial z} - \left[\bar{p}_k - \bar{p} + (\alpha_2 - \alpha_1)\left((\bar{p}_2 - \bar{p}) - (\bar{p}_1 - \bar{p})\right)\right] \frac{\partial \alpha_k}{\partial z} \quad .$$

Conventionally pressure differences are not available, so we model the first term as $-\alpha_k \frac{\partial \bar{p}}{\partial z}$. Although $\frac{\partial \alpha_k}{\partial z}$ is available as an inverse length scale in conventional models, this quantity is denoted as L^{-1}, where L is a phenomenological length and is given its own equation. On dimensional grounds, dL/dt is a velocity (difference), yielding the equation

$$dL/dt = |v_2 - v_1|_{z=0} \quad .$$

We note further that if we continue with the identification of $\partial \alpha_k / \partial z$ with L^{-1}, then the derivative of (4.5) with respect to z gives a conservation law for L^{-1}, which is not equivalent to the above ordinary differential equation.

The pressure differences above are not available in conventional models, so they must be replaced by a dimensionally equivalent term, which we take to be density times a velocity difference squared. In this substitution, an undetermined dimensionless parameter is allowed.

This completes the derivation of the usual drag model and closure assumptions from ours, at the level of rigor with which the conventional models are themselves derived. This also explains, intuitively, why our procedure does not require adjustable parameters.

To complete our system, we need an effective equation of state for each phase, but not for the mixture. We consider the internal energy ϵ_k as a function of density ρ_k and pressure p_k. We approximate the effective equation of state as

$$\tilde{\epsilon}_k = \tilde{f}_k(\rho_k, p_k) \approx f_k(\bar{\rho}_k, \bar{p}_k). \tag{4.10}$$

In this approximation, we assume that pressure and density variations within a phase are small relative to variations in these quantities between phases. In other words, the phase equation of state approximation avoids the difficulties commonly associated with defining equations of state for mixtures.

Altogether we have ten unknowns, $\alpha_k, \bar{v}_k, \bar{\rho}_k, \bar{p}_k$ and $\tilde{\epsilon}_k$ for $k = 1, 2$ and ten equations, (4.6)-(4.8), (4.10) for each phase, (4.9) and (4.5) for one of the phases. Equation (4.5) for the other phase can be derived by using (4.9). Therefore our system is closed for $0 < \alpha_k < 1$.

In order to compare the solution from the effective equations with the results from the numerical computations, we specialize the equation of state to the stiffened polytropic gas

$$\epsilon_k = \frac{p_k + \gamma_k p_{s,k}}{(\gamma_k - 1)\rho_k} \ . \tag{4.11}$$

Here γ_k is a dimensionless constant and $p_{s,k}$ is a constant with the dimension of pressure. According to our approximation for the effective equation of state, we have

$$\tilde{\epsilon}_k = \frac{\bar{p}_k + \gamma_k p_{s,k}}{(\gamma_k - 1)\bar{\rho}_k} \ .$$

Substituting this expression into the energy equation (4.8), we have

$$\frac{\partial}{\partial t}[\frac{\alpha_k(\bar{p}_k + \gamma_k p_{s,k})}{\gamma_k - 1}] + \frac{\partial}{\partial z}[\frac{\alpha_k \bar{v}_k(\bar{p}_k + \gamma_k p_{s,k})}{\gamma_k - 1}] = -\bar{p}_k \frac{\partial(\alpha_k \bar{v}_k)}{\partial z} + (\alpha_1 \bar{p}_2 \bar{v}_2 + \alpha_2 \bar{p}_1 \bar{v}_1)\frac{\partial \alpha_k}{\partial z} \quad . \qquad (4.12)$$

Actually, for the stiffened polytropic equation of state, there is no approximation at all in the effective equation of state. This is due to the fact that the internal energy appears in (4.8) as $\alpha_k \bar{\rho}_k \tilde{\epsilon}_k$.

We comment that there are no free parameters in our model. From (4.5) and the method of characteristics, it is easy to see that α_k lies between 0 and 1 for all times since α_k lies in that range initially.

The characteristic speeds of system (4.5)-(4.9) consist of the characteristic speeds $\bar{v}_k$ and $\bar{v}_k \pm c_k$ of each phase separately, together with the speed $\alpha_1 \bar{v}_2 + \alpha_2 \bar{v}_1$ for the volume fraction mode. In particular, the system has only real characteristics, and thus is hyperbolic. See also [12] for a different closure, which also has purely real characteristic speeds. From this analysis, we see that the number of independent modes and the characteristic structure of the system changes across any surface for which one of the volume fractions goes to zero. Moreover, on the two phase side of this surface (the side for which $0 < \alpha_k < 1$), there will be one incoming characteristic (of the larger system) for which there is no data, as the corresponding mode does not exist in the smaller (one phase) system on the other side of this surface. This characteristic is an incoming sound wave for the phase whose volume fraction goes to zero at the surface. In this sense, our closure is not complete, but it has reduced the closure problem from a volume to a surface condition, and given it an improved physical basis.

5 Loss of Universality for Compressible Rayleigh-Taylor Mixing

Experiments [10,14] and simulations have shown that the incompressible Rayleigh-Taylor mixing problem has a mixing region growth rate which is universal, for random initial disturbances of a flat interface. In this section, we discuss the loss of universality for compressible Rayleigh-Taylor

mixing. Universality is important theoretically, as it supports the notion of a renormalization group fixed point for this problem, and it is important practically, as it eliminates the need to characterize the detailed properties of a randomly perturbed interface. In order to compare solutions obtained with different parameter values, it is important to introduce dimensionless units. We choose dimensionless (primed) space and time units for which $g' = 1$, namely $x' = xg/c_0^2$, $t' = tg/c_0$, where c_0 is a characteristic velocity, taken here to be the sound speed of the heavy gas at the interface at time zero. In these units, $v' = v/c_0$. We also transform the mass in such a way that the density $\rho' = \rho$ is not transformed. The transformation rules for pressure, $p' = p/c_0^2$ and energy density $\tilde{\epsilon}' = \tilde{\epsilon}/c_0^2$, are then uniquely determined. The dimensionless compressibility $M = (\lambda g/c_o^2)^{1/2}$, with λ a characteristic transverse length, is written as $M = M' = (\lambda')^{1/2}$. While the Atwood number A_t is an attribute of the equations alone, M^2 refers to the solution as well as to the equations, and as dimensionalized here, has the role of a dimensionless transverse length. The random initial conditions are additionally characterized by initial amplitude, $a_0' = \delta z_0' = \delta z_0 g/c_0^2 = a_0 g/c_0^2$. Our previous studies [2] had considered $\delta z_0/\lambda = a_0'/M^2$ as a dimensionless characterization of the initial conditions, with the choice $a_0'/M^2 \ll 1$ to reduce the influence of this parameter on the solution.

Henceforth, we refer only to the dimensionless units, and drop all further reference to primes. Thus the governing equations are given as (4.5) - (4.10), with $g = 1$.

The initial conditions are determined by the linearized compressible Rayleigh-Taylor theory [5]. Assume the computational domain is a rectangle defined as $(x, z) \in [x_l, x_u] \times [z_l, z_u]$. The initial perturbed interface is given by

$$z = z_{\rm intfc} + \sum_n A_n \cos \frac{2\pi n(x - x_l)}{(x_u - x_l)}, \qquad x \in [x_l,\ x_u] \ ,$$

where $z_{\rm intfc}$ is the position of the unperturbed interface and A_n is the amplitude of the interface perturbation corresponding to mode n. We consider a random interface problem, in which A_n is chosen by using independent Gaussian variables. The detailed choice of A_n is described in [2]. Note that the long wave length modes are set to zero. Let $L = |x_u - x_l|$, then

$$\alpha_1(z,\ 0) \ = \ \frac{1}{L} \sum_{ensemble} \int_{x_l}^{x_u} \Theta(z - z_{\rm intfc} - \sum_n A_n \cos \frac{2\pi n(x - x_l)}{(x_u - x_l)})\ dx \ ,$$

and

$$\alpha_2(z,\ 0) \ = \ 1 \ - \ \alpha_1(z,\ 0) \ ,$$

where Θ is the Heaviside function.

Our results suggest the following RNG interpretation. The Rayleigh-Taylor mixing dynamics is a flow away from an unstable RNG fixed point, defined by the unstable unperturbed flat interface,

towards a possible one parameter family of fixed points. This family is determined as follows: the convention that (a) low wave numbers are eliminated and (b) the remaining modes have equal weights, defines a distinguished one parameter family of random initial conditions labeled by an overall amplitude. In this family, the time $t = 0$ is uniquely fixed by the equal weight hypothesis on the allowed modes.

Let a_0 denote the variance of the Gaussian random variable which defines the A_n. Thus a_0 parameterizes the initial conditions. The resulting family of solutions can also be understood in terms of data at times $t_0 \neq 0$. If the amplitude is still small, the time propagation from $t = 0$ to $t = t_0$ will be given by the linear theory. At $t = t_0$, the Fourier modes in the interface will not be equally weighted. For example if $t_0 < 0$, the $t = t_0$ amplitudes will be smaller, but the longer of the allowed wave lengths will be exponentially larger in relative amplitude. Thus the one parameter family of initial measures on function space could alternately be described in terms of a constant amplitude, but with a variable exponentially weighted relative amplitude for the allowed modes.

Additionally, we require a small amplitude to wavelength restriction, $a_0 \ll \lambda$, for validity of the linear perturbation theory used to define the initial conditions at $t = 0$. Since $M^2 = \lambda$ is a dimensionless transverse length, the incompressible limit $M^2 \to 0$ forces $a_0 \to 0$, giving a unique solution from our one parameter family in the incompressible limit.

Our previous nondimensionalization of initial conditions was in terms of the validity of linear perturbation theory, *i.e.* $a_0/\lambda = a_0/M^2 \ll 1$. For the long time dynamics, a_0 is a better description of the initial data than is a_0/M^2. In fact for the ensembled averaged equations, λ and M^2 are not defined, and all transverse degrees of freedom have been eliminated, while a_0 retains its meaning. Our earlier direct simulation data can be replotted in the dimensionless units used here.

We find that the previously observed dependence on M^2 can be seen as a dependence on the initial amplitude a_0. More fundamentally, the observed dependence on M^2 can be seen as a dependence on the relative strength of the moderate and high frequency modes in the random initial data. From this point of view, there should be no RNG fixed point for compressible Rayleigh-Taylor mixing, other than by approximation to the incompressible limit.

6 Conclusions

Two phase turbulent mixing data, obtained from direct numerical simulation of the two fluid Euler equations by the front tracking method, was analyzed.

A new two phase closure, with no adjustable parameters, is proposed. The closure is validated

by comparison with simulation data, which, itself is in agreement with experiment. The closure is not complete, as there is a missing condition along the internal boundaries for which one phase goes to zero volume fraction. The closure also provides a qualitatively new insight into the previously reported compressibility dependent mixing rate. The latter is now seen as a dependence on initial amplitude, which becomes a more natural occurrence in a highly compressible situation. Both turbulent and two phase formulations were considered. The two phase formulation appears to be more satisfactory. For example, products of the first moments of the two phase formulation reproduce the second moments of the turbulent formulation correctly.

References

1. Besnard, D., Harlow, F. and Rauenzahn, R. *Conservation and Transport Properties of Turbulence with Large Density Variations.* LANL report LA-10911-MS, 1990.
2. Chen, Y., Deng, Y., Glimm, J., Li, G., Sharp, D. H. and Zhang, Q. *A Renormalization Group Scaling Analysis For Compressible Two-Phase Flow. Phys. Fluids A 5* 11 (1993), 2929–2937.
3. Drew, D. A. *Mathematical Modeling of Two-phase Flow. J. Fluid Mech. 86* (1983), 261–291.
4. Freed, N., Ofer, D., Shvarts, D. and Orszag, S. *Two-phase Flow Analysis of Self-similar Turbulent Mixing by Rayleigh-Taylor Instability. Physics of Fluids A 35* (1991), 912–918.
5. Gardner, C. L., Glimm, J., McBryan, O., Menikoff, R., Sharp, D. and Zhang, Q. *The Dynamics of Bubble Growth for Rayleigh-Taylor Unstable Interfaces. Phys. of Fluids 31* (1988), 447–465.
6. Glimm, J. and Li, X. *On the Validation of the Sharp-Wheeler Bubble Merger Model from Experimental and Computational Data. Phys. Fluids 31* (1988), 2077–2085.
7. Glimm, J., Li, X. L., Menikoff, R., Sharp, D. H. and Zhang, Q. *A Numerical Study of Bubble Interactions in Rayleigh-Taylor Instability for Compressible Fluids. Phys. Fluids A* 211 (1990), 2046–2054.
8. Harlow, F. and Amsden, A. *Flow of Interpenetrating Material Phases. J. Comp. Phys. 18* (1975), 440–464.
9. Miksis, M. J. and Ting, L. *Effective Equations for Multiphase Flows–Waves in a Bubbly Liquid. Advances in Applied Mechanics 28* (1992), 141–260.

10. Read, K. I. *Experimental Investigation of Turbulent Mixing by Rayleigh-Taylor Instability. Physica D 12* (1984), 45.

11. Sharp, D. H. *An Overview of Rayleigh-Taylor Instability. Physica D 12* (1984), 3–18.

12. Stewart, H. B. and Wendroff, B. *Two-Phase Flow: Models and Methods. J. Comp. Phys. 56* (1984), 363–409.

13. Tryggvason, G. *Numerical Simulations of the Rayleigh-Taylor Instability. J. Comp. Phys. 752* (1988), 253–282.

14. Youngs, D. L. *Numerical Simulation of Turbulent Mixing by Rayleigh-Taylor Instability. Physica D 12* (1984), 32–44.

7 Captions

Figure 2.1. (a) Comparison between the exact value and two phase approximate value of B (equations (2.2a) and (2.5a)) for $t = 2, 5, 7$ and 9. (b) Comparison between the exact value and two phase approximate value of A (equations (2.2b) and (2.5b)) for $t = 2, 5, 7$ and 9. Here the Atwood number is $A_t = 2/3$ and the dimensionless compressibility $M^2 = 0.5$. We see that the approximation is in very close agreement with the exact correlations for A and B.

Figure 2.2. Comparison between the exact value and two phase approximate value of R (equations (2.2c) and (2.5c)) for $t = 0, 6, 9$ and 11. Although the agreement is not as good as that shown in Figure 2.1 for A and B the approximation still correctly captures most of the contribution to R.

Figure 2.3. (a) Comparison between the exact value of S and two phase approximate value $S_{\text{two phase}}$ for $t = 2, 5, 7$ and 9. (b) Comparison between the exact value of G and the two phase approximate value $G_{\text{two phase}}$ for $t = 2, 5, 7$ and 9. Here the Atwood number is $A_t = 2/3$ and the dimensionless compressibility $M^2 = 0.5$. We see that the approximation is in very close agreement with the exact correlations for S and G.

Figure 3.1. Comparison between $\langle p \nabla X_k \vec{v}_k \rangle$ and $\bar{p}_k \nabla \cdot (\alpha_k \bar{v}_k)$ for $A_t = 2/3$ and $M^2 = 0.5$. 3.1(a) shows the result for phase 1 at times $t = 5$ and 9 and 3.1(b) gives the result for phase 2 at times $t = 2$ and 8. Since the quantities shown here are quite close to each other, the correlation term derived in the averaged equation for the energy is negligible.

Figure 4.1. Comparison between $\langle \vec{v}_{\text{int}} \cdot \nabla X_k \rangle$ and $(\alpha_1 \bar{v}_2 + \alpha_2 \bar{v}_1) \cdot \nabla \alpha_k$ for $A_t = 2/3$ and $M^2 = 0.5$ at times $t = 3, 6, 9$ and 12. The solid curves correspond to the exact expression $\langle \vec{v}_{\text{int}} \cdot \nabla X_k \rangle$ and the dashed curves are the results obtained from the one-dimensional model $(\alpha_1 \bar{v}_2 + \alpha_2 \bar{v}_1) \cdot \nabla \alpha_k$. The agreement is surprisingly good.

Figure 4.2. Comparison between $\langle p \nabla X_k \rangle$ and $(\alpha_1 \bar{p}_2 + \alpha_2 \bar{p}_1) \cdot \nabla \alpha_k$ for $A_t = 2/3$ and $M^2 = 0.5$ at times $t = 3, 6, 9$ and 12. The solid curves correspond to the exact expression $\langle p \nabla X_k \rangle$ and the dashed curves are the results obtained from the one-dimensional model $(\alpha_1 \bar{p}_2 + \alpha_2 \bar{p}_1) \cdot \nabla \alpha_k$. The agreement is remarkably good over the entire mixing zone.

Figure 4.3. Comparison between $\langle p \vec{v} \cdot \nabla X_k \rangle$ and $(\alpha_1 \bar{p}_2 \bar{v}_2 + \alpha_2 \bar{p}_1 \bar{v}_1) \cdot \nabla \alpha_k$ for $A_t = 2/3$ and $M^2 = 0.5$ at times $t = 3, 6, 9$ and 12. The solid curves correspond to the exact expression $\langle p \vec{v} \cdot \nabla X_k \rangle$ and the dashed curves are the results of the one-dimensional model $(\alpha_1 \bar{p}_2 \bar{v}_2 + \alpha_2 \bar{p}_1 \bar{v}_1) \cdot \nabla \alpha_k$. The agreement is surprisingly good. This figure is quite similar to Figure 4.2, because the error comes mainly from the approximation to the velocity of the interface.

Figure 4.4. Comparison between $\tilde{v}_k$ and $\bar{v}_k$ for $A_t = 2/3$ and $M^2 = 0.5$ at times $t = 2, 5, 7$ and 9. 4.4(a) shows the results for phase 1 and 4.4(b) gives the results for phase 2. This plot shows that the results obtained from the volume average and the density average are nearly the same.

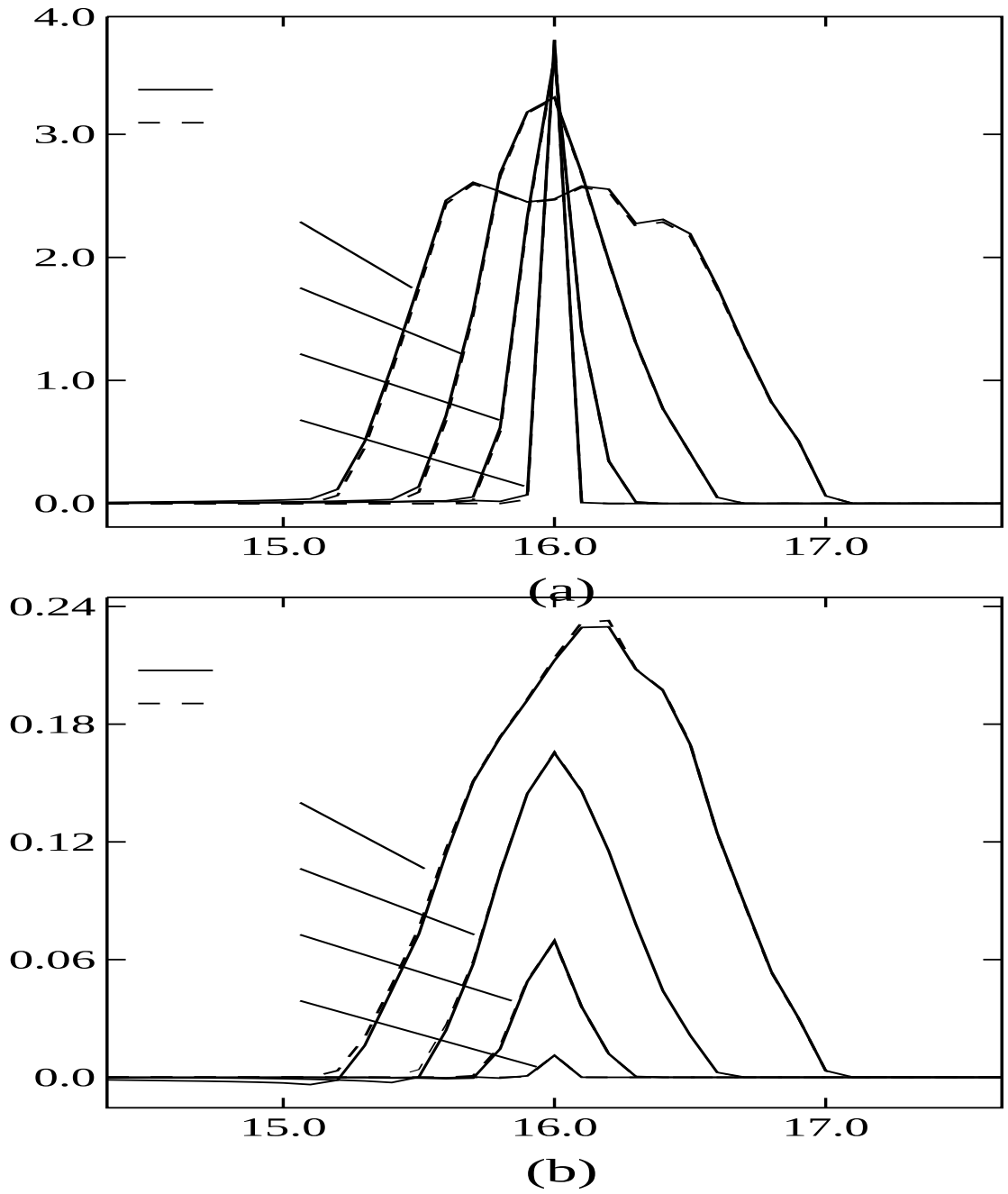

Figure 2.1. (a) The comparison between the exact value and two phase approximate value of B (equations (2.2a) and (2.5a)) for $t = 2, 5, 7$ and 9. (b) The comparison between the exact value and two phase approximate value of A (equations (2.2b) and (2.5b)) for $t = 2, 5, 7$ and 9. Here the Atwood number is $A_t = 2/3$ and the dimensionless compressibility $M^2 = 0.5$. We see that the approximation is very close to the exact correlation for A and B.

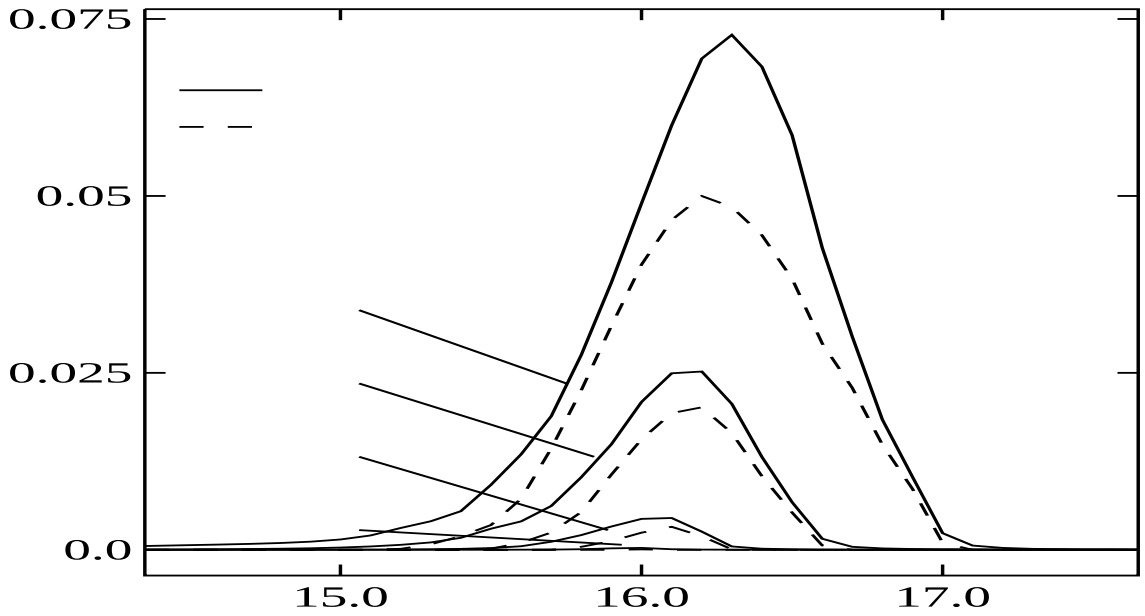

Figure 2.2. The comparison between the exact value and two phase approximate value of R (equations (2.2c) and (2.5c)) for $t = 0, 6, 9$ and 11. Although the agreement is not as good as the ones shown in Figure 2.1 for A and B, it still captures most of the contribution to R.

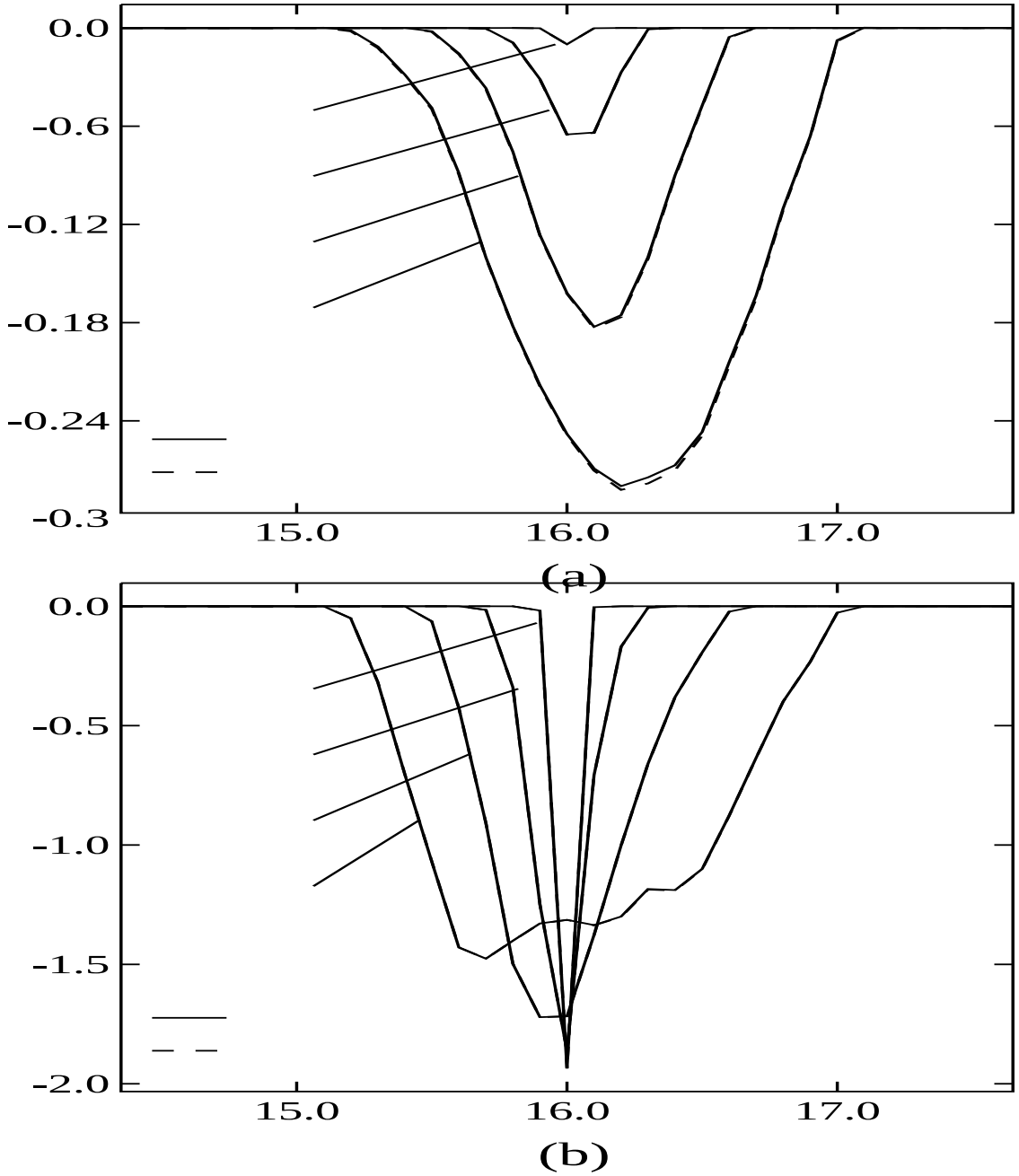

Figure 2.3. (a) The comparison between the exact value S and two phase approximate value $S_{\text{ two phase}}$ for $t = 2, 5, 7$ and 9. (b) The comparison between the exact value G and two phase approximate value $G_{\text{ two phase}}$ for $t = 2, 5, 7$ and 9. Here the Atwood number is $A_t = 2/3$ and the dimensionless compressibility $M^2 = 0.5$. We see that the approximation is very close to the exact correlation for S and G.

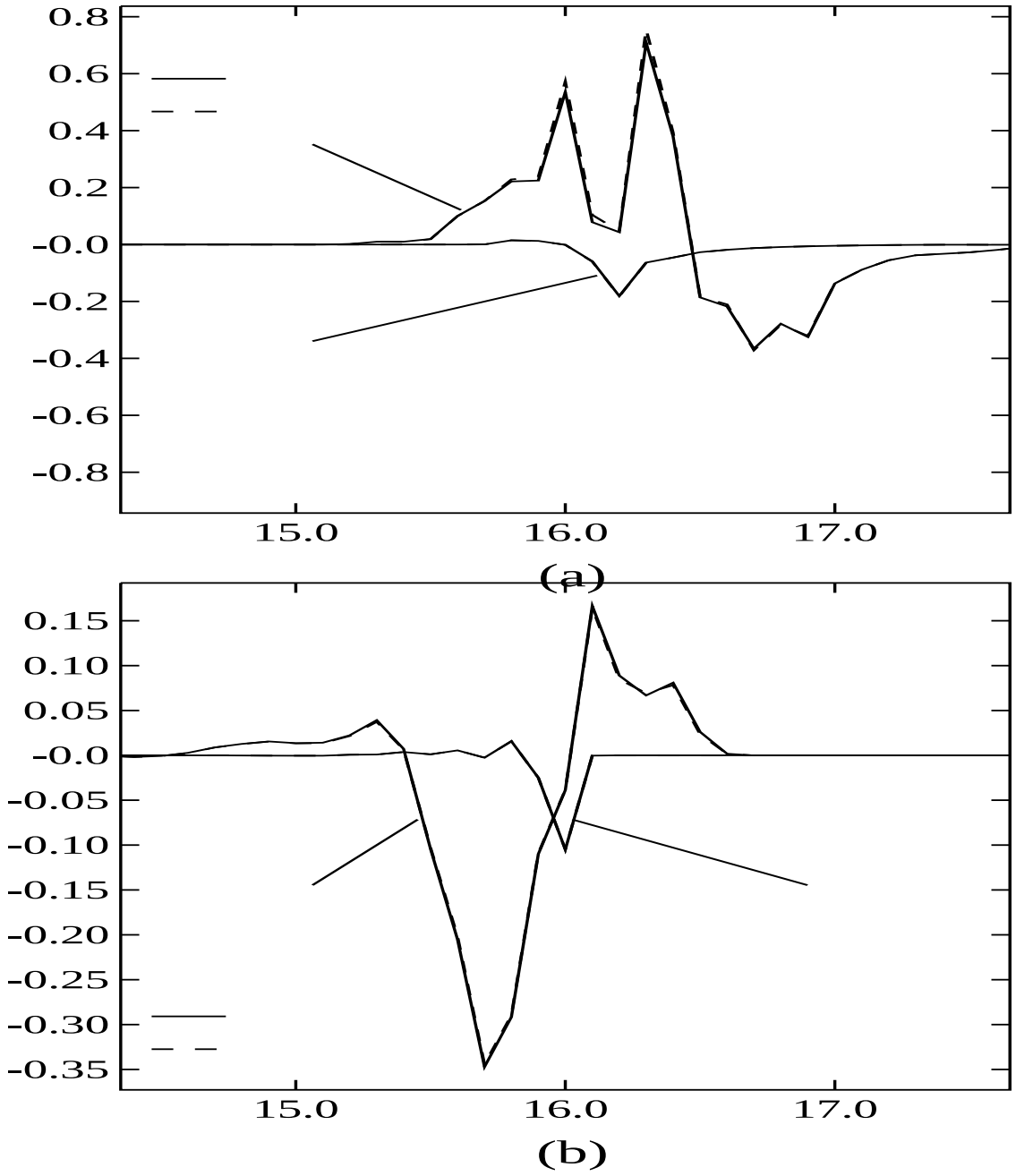

Figure 3.1. The comparison between $\langle p\nabla X_k \vec{v}_k \rangle$ and $\bar{p}_k \nabla \cdot (\alpha_k \bar{v}_k)$ for $A_t = 2/3$ and $M^2 = 0.5$. (a) is for phase 1 at times $t = 5$ and 9 and (b) is for phase 2 at times $t = 2$ and 8. Since the quantities shown here are quite close to each other, the correlation term derived in the averaged equation for energy is negligible.

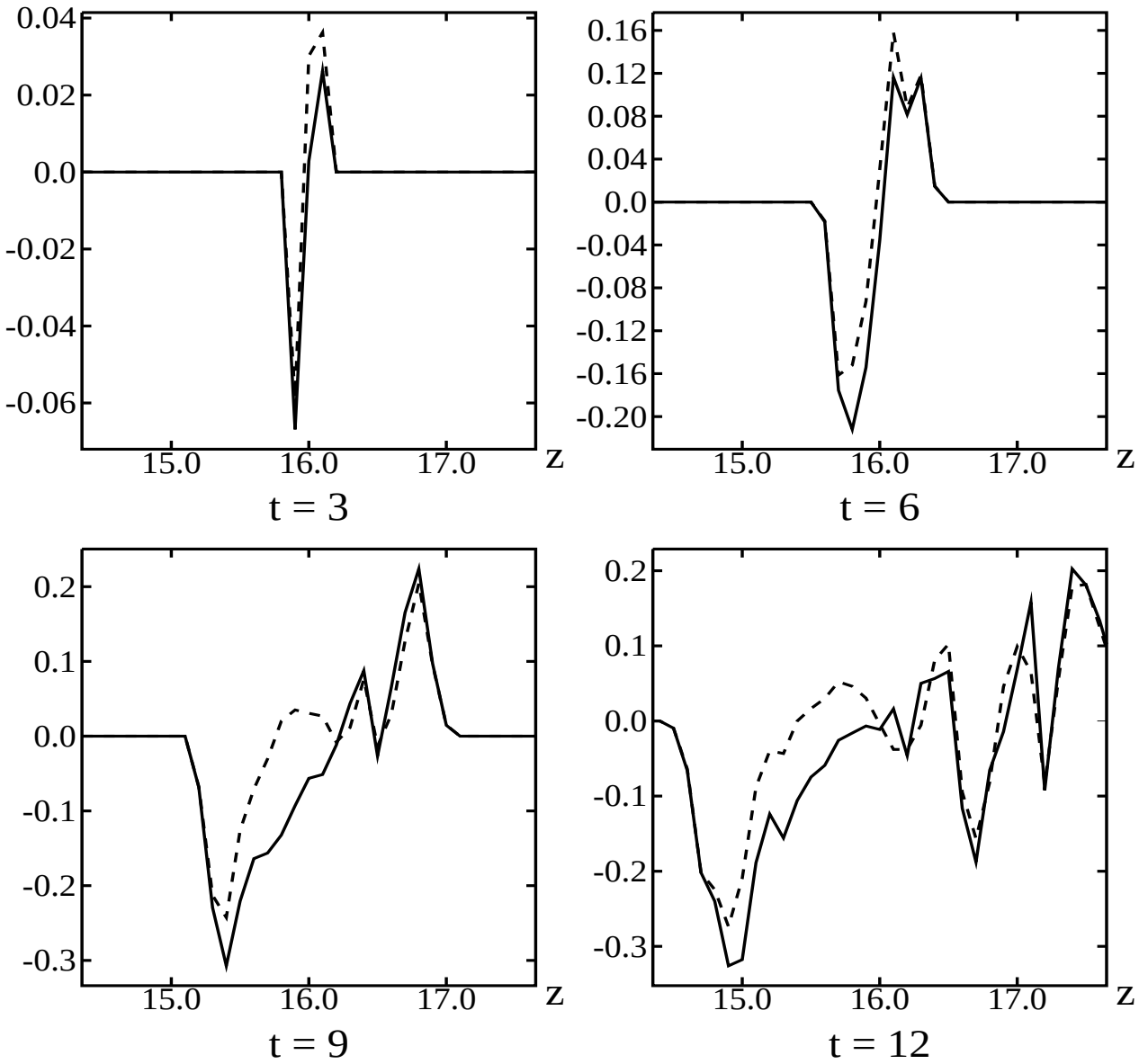

Figure 4.1. The comparison between $\langle \vec{v}_{\rm int} \cdot \nabla X_k \rangle$ and $(\alpha_1 \bar{v}_2 + \alpha_2 \bar{v}_1) \cdot \nabla \alpha_k$ for $A_t = 2/3$ and $M^2 = 0.5$ at times $t = 3, 6, 9$ and 12. The solid curves are the results of the exact expression $\langle \vec{v}_{\rm int} \cdot \nabla X_k \rangle$ and the dashed curves are the results of the one-dimensional model $(\alpha_1 \bar{v}_2 + \alpha_2 \bar{v}_1) \cdot \nabla \alpha_k$. The agreement is very good near the edges of the mixing zone. At the center of the mixing zone, the approximation still capture the qualitative features of the original data.

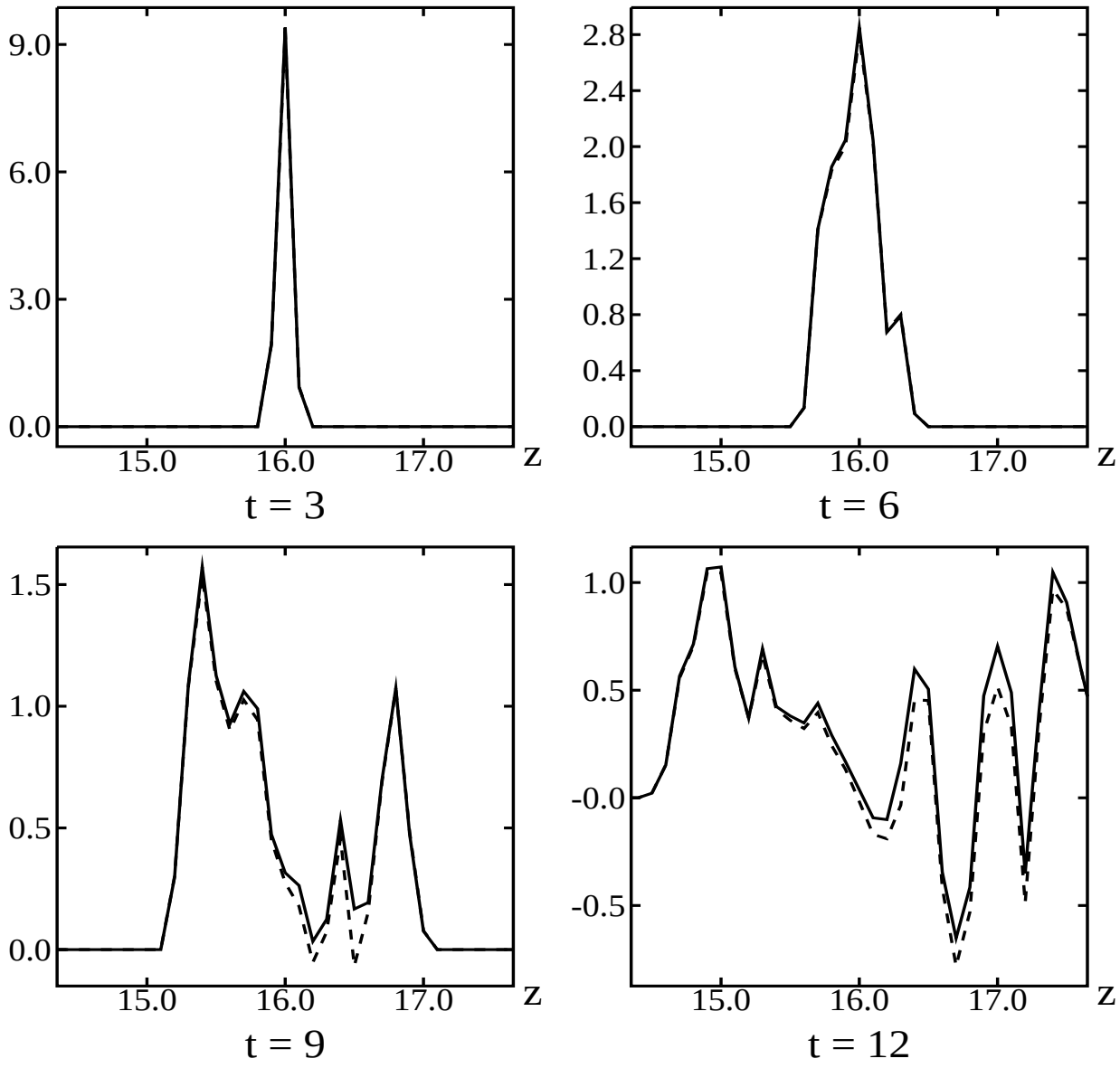

Figure 4.2. The comparison between $\langle p\nabla X_k\rangle$ and $(\alpha_1\bar{p}_2+\alpha_2\bar{p}_1)\cdot\nabla\alpha_k$. for $A_t=2/3$ and $M^2=0.5$ at times $t = 3,6,9$ and 12. The solid curves are the results of the exact expression $\langle p\nabla X_k\rangle$ and the dashed curves are the results of the one-dimensional model $(\alpha_1\bar{p}_2+\alpha_2\bar{p}_1)\cdot\nabla\alpha_k$. The agreement is very good over the whole mixing zone.

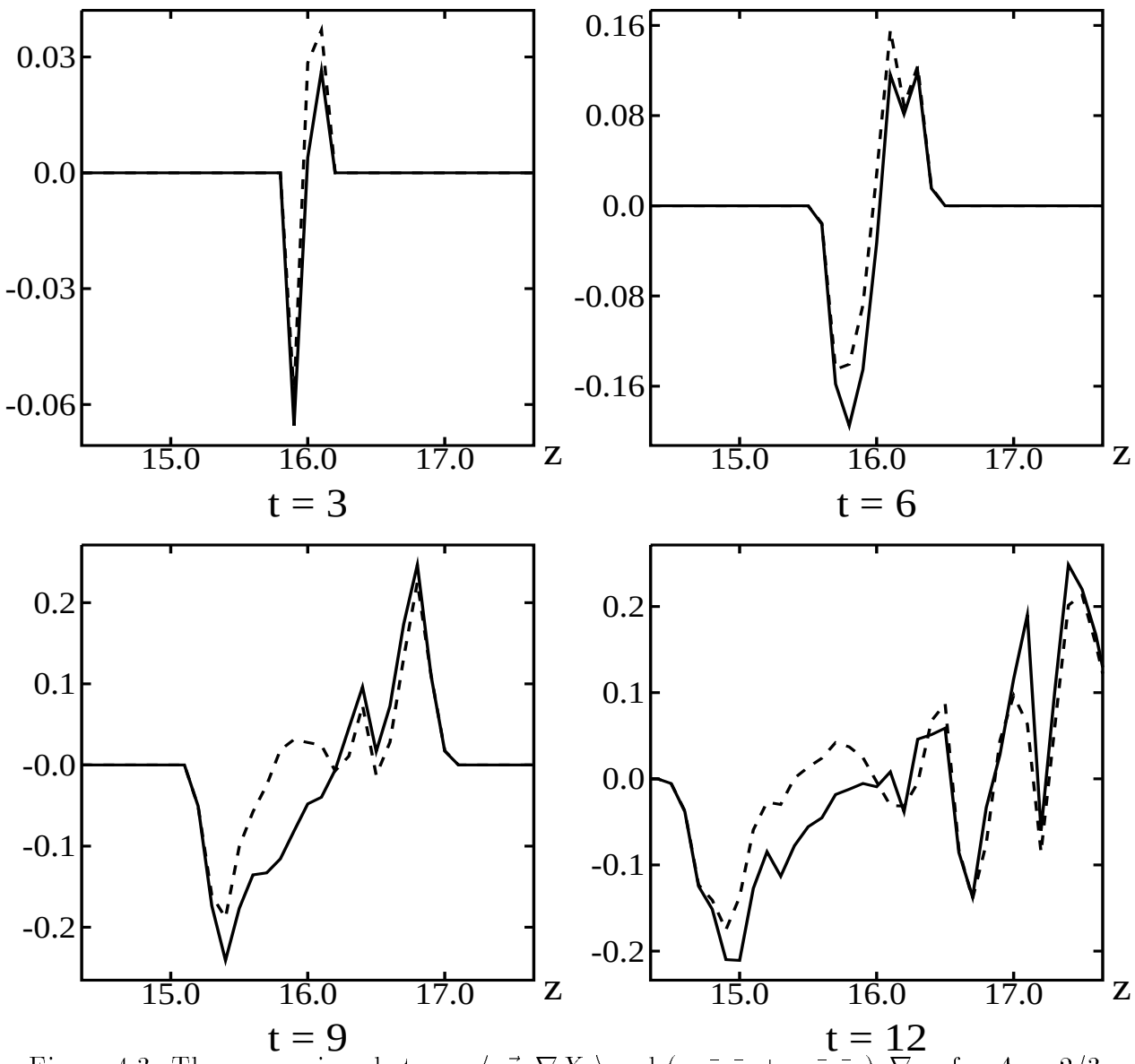

Figure 4.3. The comparison between $\langle p\vec{v}\cdot\nabla X_k\rangle$ and $(\alpha_1\bar{p}_2\bar{v}_2+\alpha_2\bar{p}_1\bar{v}_1)\cdot\nabla\alpha_k$ for $A_t = 2/3$ and $M^2 = 0.5$ at times $t = 3, 6, 9$ and 12. The solid curves are the results of the exact expression $\langle p\vec{v}\cdot\nabla X_k\rangle$ and and the dashed curves are the results of the one-dimensional model $(\alpha_1\bar{p}_2\bar{v}_2 + \alpha_2\bar{p}_1\bar{v}_1)\cdot\nabla\alpha_k$. The agreement is very good near the edges of the mixing zone. At the center of the mixing zone, the approximation still capture the qualitative features of the original data. This figure is quite similar to figure 4.2, because the error mainly comes from the approximetion to velocity of the interface.

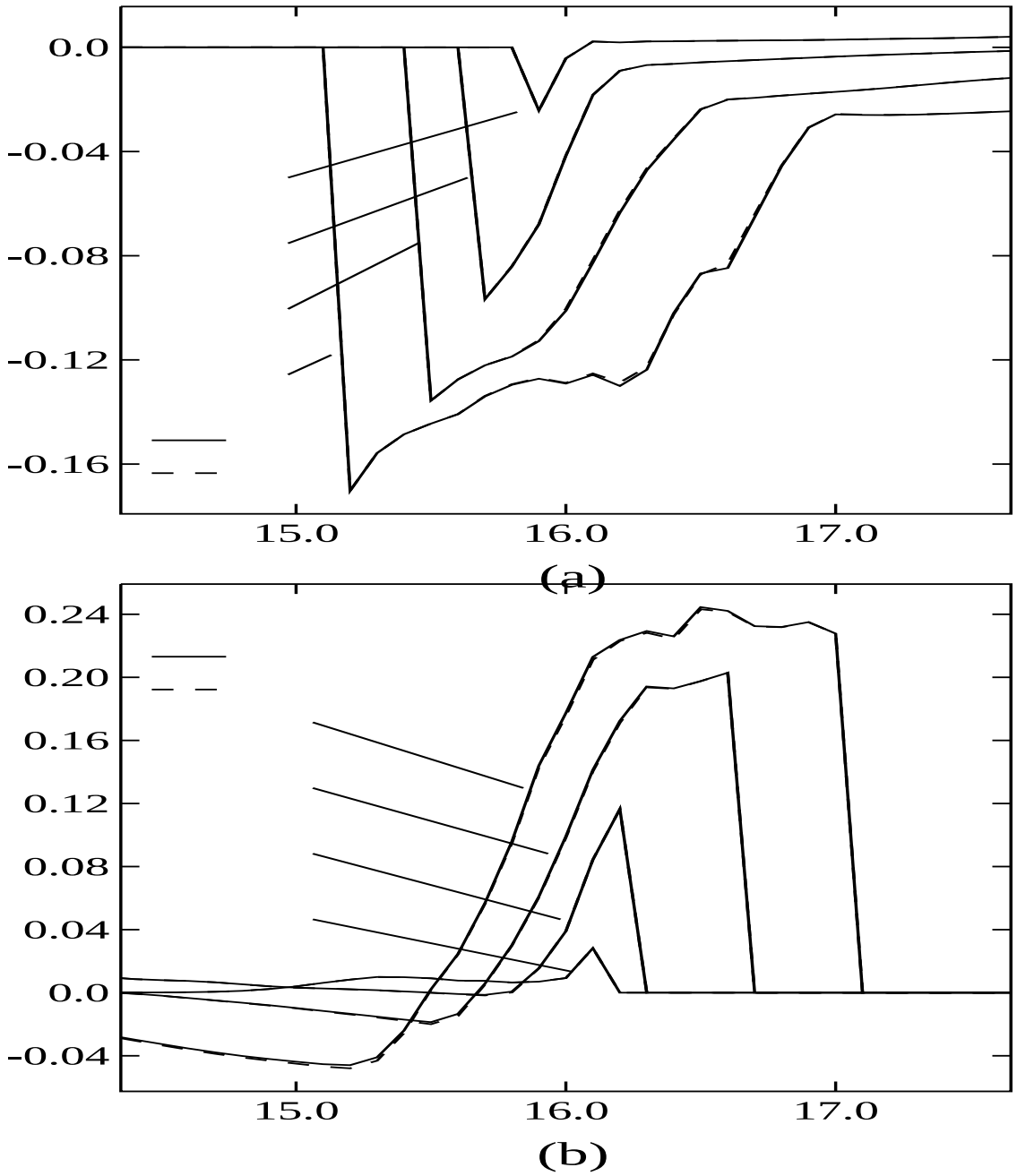

Figure 4.4. The comparison between $\tilde{v}_k$ and $\bar{v}_k$ for $A_t = 2/3$ and $M^2 = 0.5$ at times $t = 2, 5, 7$ and 9. (a) is for phase 1 and (b) is for phase 2. It shows that the result from the volume average and the result from the density average are almost the same.